PAPER • OPEN ACCESS

Design of a small pressure chamber to evaluate probe calibrations at varying Reynolds numbers

View the article online for updates and enhancements.

You may also like

- The development of a -biomimetic uncooled IR-Sensor inspired by the infrared receptors of *Melanophila acuminata*
Georg Siebke, Peter Holik, Sam Schmitz et al.

- Optical Emission Spectroscopy Study of the Electron Temperature and Electron Density Dependence on the Pressure Chamber for the Carbon Deposition Produced by Argon Plasma Sputtering
D R S Pambudi, M A Hanif, D J D H Santjojo et al.

- Spectral characteristics of underwater laser-induced breakdown spectroscopy under high-pressure conditions
Lintao WANG, , Ye TIAN et al.

Design of a small pressure chamber to evaluate probe calibrations at varying Reynolds numbers

K Speck, C Schäffer and V Gümmer

Technical University of Munich, TUM School of Engineering and Design, Chair of Turbomachinery and Flight Propulsion
Boltzmannstraße 15, 85748 Garching bei München, Germany

E-mail: `konstantin.speck@tum.de`

Abstract. The Chair of Turbomachinery and Flight Propulsion (LTF) at the Technical University of Munich (TUM) operates a wind tunnel for probe calibration (Caljet). This paper describes the design and the validation process of a pressure chamber. The pressure chamber is used to calibrate probes for turbomachinery applications at comparable conditions to a 3.5-stages axial compressor test rig. This allows the study of Reynolds number and Mach number effects individually. The pressure chamber is designed as an additional component for the Caljet to enable probe calibration at higher mass flow densities and higher Reynolds numbers. Therefore, the original free stream jet is encased by this chamber, nevertheless the outlet of the calibration wind tunnel remains open to the environment. After a first pre-design study, numerical simulations are carried out to confirm expected flow conditions in the measurement area. Ansys Fluent is used for RANS simulations with air modeled as compressible gas. The numerical results are validated with experimental investigations that simultaneously provide a deeper understanding of the flow behavior. Therefore, a five-hole probe, a hot-wire probe, and a Fast Response Aerodynamic Probe are utilized. It is shown that the capability of the jet meets the expectations and can be used for the calibration of hot-wire probes at conditions comparable to a state-of-the-art 3.5-stages axial compressor.

1. Introduction

A detailed understanding of the flow physics and aerodynamic loss mechanisms within turbomachinery is still an ongoing challenge. Therefore, probes with a high spatial and temporal resolution are utilized to resolve the flow within LTF´s High-Speed Research Compressor (HSRC) at the TUM. The test vehicle is equipped with several traversing slots which enable the investigation of the flow within a modern high-pressure compressor rear stage concept. The applied probes such as

- five-hole probes (5HP),
- total temperature and total pressure Kiel-probes (T_t-Kiel probe),
- Fast-Response Aerodynamic Probes (FRAP),
- and hot-wire probes (HW)

are calibrated under steady-state conditions in a calibration tunnel with respect to yaw and pitch angle, Mach number, and total temperature.

During the calibration of the HW probes, a permanent wire breakage occurred when exceeding a certain Mach number, which may be related to wire vibrations, also discovered by Boyle et al. [1] However, the pressure chamber permits the calibration of the HW probes at moderate Mach numbers but at higher mass flow densities by increasing the static pressure inside the chamber. Therefore, the pressure chamber enables to calibrate a probe at the same steady conditions in terms of Mach number, total temperature, and mass flow density as in the research compressor. Gieß et al describes in [2] a new test facility for probe calibration, which allows independent variation of Mach and Reynolds numbers. The complex setup and good equipment provide a large working range. This probe calibration wind tunnel is mainly used to calibrate pressure probes.

Furthermore, a preliminary numerical investigation by Schäffer et al [3] yields a small dependency of the Reynolds number on the calibration of a five-hole probe. An experimental analysis is necessary to prove the numerical results at lower over pressure. Therefore, this pressure chamber concept is designed to vary the Mach and Reynolds number independently in a range from ambient pressure up to 2250 hPa absolute pressure and Mach numbers from Ma $= 0, 05$ to Ma $= 0, 95$.

2. Design

As described before, the pressure chamber is adapted to an existing calibration wind tunnel. The design aims to extend the capability from free stream calibrations to calibrations at higher ambient pressure. Therefore, the pressure chamber is designed with a plug-and-play principle to mount and demount the chamber in a short time.

Wind tunnel

The existing wind tunnel is a free stream wind tunnel. The air is provided via different systems, depending on the required temperature and Mach number. For low Mach numbers and no temperature dependence, two different blowers can be used, depending on the required Mach number. Higher Mach numbers are realized with the 13 bar shop air supply that has sufficient large compressors and pressure tanks. Since raising the ambient pressure goes hand in hand with throttling up the flow inside the pressure chamber, all investigations with the pressure chamber require the 13 bar pressure system. The simplified schematic setup is shown in Figure 1.
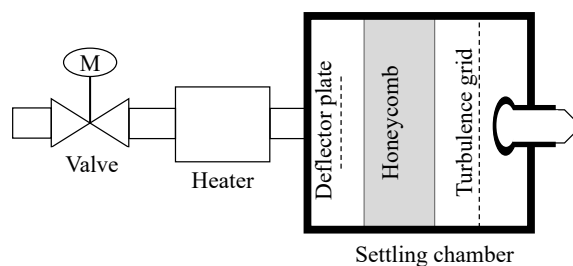

Figure 1. Schematic setup of existing wind tunnel.

An electronic valve is used to control the supply pressure from the pressure system. A 18 kW heater heats up the flow by $\Delta T_{heater,max} = 100$ K at a mass flow up to $\dot{m}_{max,heater} = 0.2\,\mathrm{kg/s}$ and a maximum differential pressure of 1250 hPa. The settling chamber has a diameter of $D_{settling\,chamber} = 500$ mm and a length of $L_{settling\,chamber} = 1000$ mm. It is isolated with a 30 mm thick high-temperature resistant isolation material. To generate a homogeneous flow field, a deflector plate, honeycomb, and a screen are placed inside the settling chamber. After a throat, a nozzle is mounted to accelerate the flow to the required Mach number. Depending on the probe head dimensions, three different nozzle sizes are available with a diameter of

$D_{Nozzle} = 25$ mm, 35 mm, and 42 mm. Small probes still can be calibrated with the 25 mm nozzle up to very high Mach numbers with the blower that enables easier control of the flow velocity. Around the nozzle, a traversing system is installed to rotate the probes for an unlimited yaw angle and a pitch angle range of $\pm 35°$.

Pressure chamber

The existing free stream calibration tunnel is adapted to become a closed measuring section calibration tunnel. To allow the calibration of hot-wire probes, precise knowledge of the total temperature is necessary. Therefore, a second probe slot for a total temperature Kiel probe next to the slot for the HW is required. Eckelmann showed in [4] that the static pressure in flow direction changes due to a change in the boundary layer thickness, which has to be considered. Further requirements include setting up a design that can be used via remote, is automated as far as possible, and has sufficient safety control. The propagated design is shown in Figure 2.

The pressure chamber has an inner diameter of $d_{in} = 150$ mm. The length between the nozzle outlet to the contraction area is defined as $L_{pressure\,chamber} = 180$ mm. The contraction area creates a transition from the $d_{in} = 150$ mm to $d_{tubing} = 75$ mm with a $20°$ angle. This is necessary to connect the chamber to the tubing downstream and the following throttle valve. The measuring positions of the static pressure are located at 10 mm intervals from -10 mm to 80 mm in the axial direction relative to the outlet of the nozzle. The static pressure measurement uses the average over two circumferential positions for each axial position. At the axial positions 30 mm and 50 mm downstream of the nozzle, where the main calibration area is located, as much as three circumferential distributed measurement points are available for the static pressure. Up to two probes can be placed in parallel between the nozzle outlet and 80 mm downstream from the nozzle. For each axial position, an individual mounting plate (cf. Figure 5(4)) has to be manufactured to ensure proper sealing. During HW probe calibrations, a T_t-Kiel probe is mounted off-center and slightly shifted behind the HW probe to prevent any influence of the potential field of the Kiel probe head on the HW (cf. Figure 3).
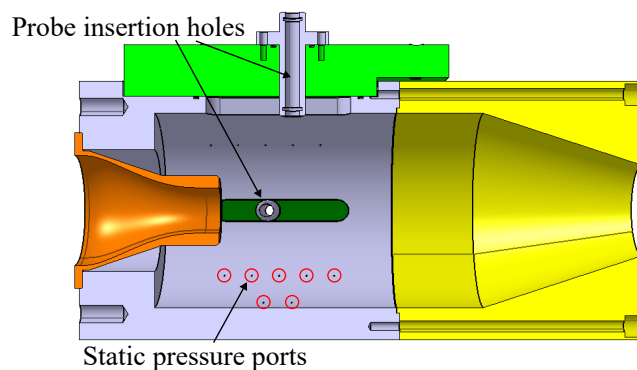

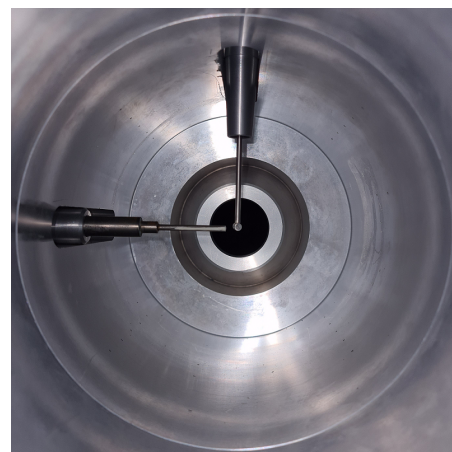**Figure 2.** Design of the pressure chamber.

Figure 3. Two probes mounted inside the pressure chamber.

Figure 4 depicts an overview over the complete setup of the pressure chamber including the Caljet. It can be seen relative to Figure 1 that merely a single adapted part has been added at the outlet of the nozzle.

Figure 5 illustrates the whole pressure chamber setup. The components are described as follows: A vertical slide with a rotational table (2) enables free movement in the yaw and radial
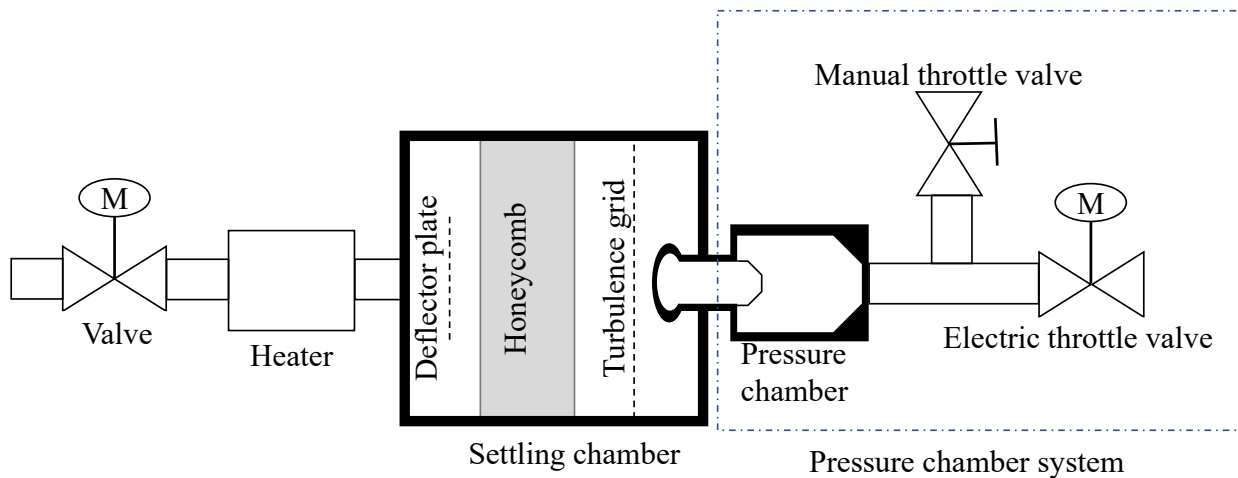
Figure 4. System configuration of pressure chamber.

directions. An automated variation of the pitch angle is not possible, since the small design dosen't allow a sealing for higher pressures while pitching. Therefore, one can insert a wedge between the mounting plate (4) and the pressure chamber (1) that tilts the mounting plate, providing a certain pitch angle. To ensure the sealing between the pressure chamber and the probe, a probe guidance (3) is manufactured which the probe is slid through. Two O-rings at the top and the lower side seal the guidance to the probe. For every probe diameter, a probe guidance must be manufactured. Probes with a diameter of up to 12 mm can be used in the pressure chamber. Downstream from the outlet of the pressure chamber, a two-meter-long metal tube is mounted to settle the flow (not shown in the picture). A tee (6) is placed downstream from the conditioning tube. On one side, a manual valve (5) is placed for a coarse adjusting of the degree of throttling and also to prevent the calibration tunnel from overpressure in case the electric valve (7) has a malfunction and closes completely. On the other side, a electric control valve (7) is placed to allow for full remote capability and also a precise adjustment of the mass flow.
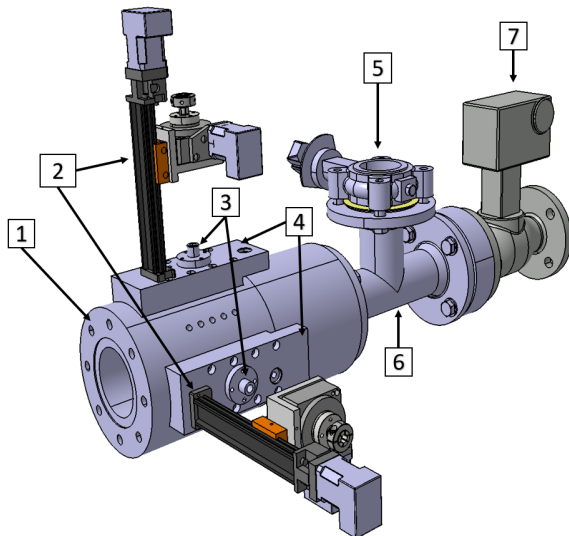

Figure 5. Detailed configuration of pressure chamber.

3. Numerical investigation

A numerical simulation is carried out to confirm that the measurement area is not influenced by any effects of the geometry of the pressure chamber. Ansys Fluent 2021 R2 is used in combination with Fluent Meshing for the simulations. All simulations are conducted on a local workstation with 16 physical cores. Small simplifications to the geometry are made in areas not affecting the main flow, e.g. the cavities for inserting the probe are not modeled. The inlet boundary condition is defined by the total pressure and total temperature. The outlet boundary condition is set by the mass flow. The outlet is moved in axial direction to obtain better conditioning of the flow and stabilize the numerical simulation. The SST turbulence model is used, air is defined as a compressible ideal gas and the energy equation is resolved. A mesh independence study yields that a mesh with 11 Mio. cells is of adequate size to get reliable results. The flow at the walls is resolved and the maximum $y+ = 1.2$. The overall calculation time is roughly 11 h. The aim of the simulation is to check the behavior of the main flow. Table 1 displays an overview of the simulation settings.

Table 1. Simulation settings.

Turbulence model	SST
Ambient pressure	96450 Pa
Inlet total pressure (relative)	80224 Pa
Inlet total temperature	293 K
Inlet turbulent intensity	0.8 %
Outlet mass flow	0.2223 kg/s
Nozzle diameter	35 mm
Fluid	Air
Density	Compressible, ideal gas

Figure 6 is shows the Mach number distribution in the axial-radial plane. It can be seen that the main flow is not deflected by the pressure chamber.
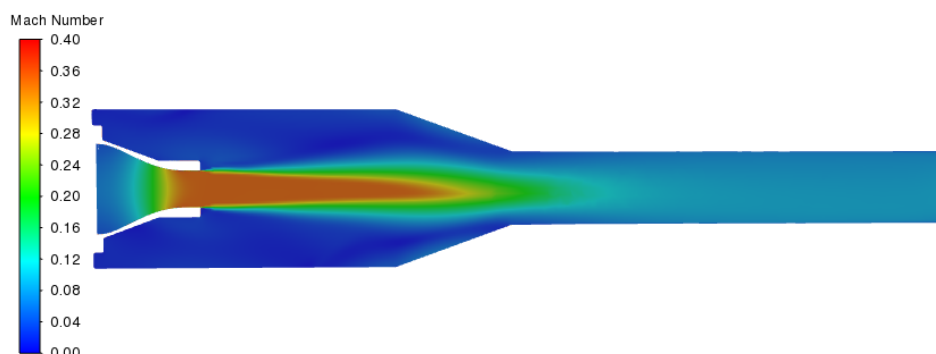

Figure 6. Distribution of Mach number.

4. Experimental investigation

To validate the numerical results, experimental investigations are conducted. The regulation of the flow conditions is complex since a change in the static pressure by throttling up the pressure chamber with (5) and (7) in Figure 5 also induces a decrease in the Mach number and vice versa. Therefore the valve in Figure 1 must be adjusted, which again changes the conditions within the pressure chamber. Additionally, a change in the flow temperature similarly causes deviations. This requires an iterative procedure until the desired Mach number, mass flow density, and temperature are finally set. The following results show data of the probe installed at 30.9 mm behind the outlet of the nozzle. At first, the flow with and without the pressure chamber mounted at the Caljet is compared for a completely unthrottled flow. The tests without the pressure chamber are conducted with only the blue-grey part in Figure 2 installed, in order to keep the probe in the exact same position and obtain identical traversing capabilities.

Turbulence measurement

Table 2 shows the Turbulent Intensity (TI) for tests with and without pressure chamber measured with HW and FRAP. The TI calculated via HW is based on the principle presented by Boufidi et al [5] discribed in Equation (1):

$$TI = \frac{\overline{v\prime}}{\overline{\overline{V}}} \tag{1}$$

$\overline{V}$ is the mean velocity of the flow in flow direction, as a wire is utilized. $\overline{v\prime}$ represents the square root of the variance hence, the root-mean-square of the velocity fluctuations. The Turbulence Intensity measured with a 2-sensor-FRAP is calculated in accordance with the approach from Hinze [6]. As seen in Table 2, the TI is in close agreement for all methods across all tests. Only the TI for the FRAP measurements using the pressure chamber is slightly higher. It has to be considered that the uncertainty for calculating the TI from the FRAP data is higher. Nevertheless, the overall TI is relatively high for a probe calibration wind tunnel due to the geometry and small number of screens in the settling chamber.

Table 2. Turbulent Intensity at Ma = 0.4.

Configuration	Turbulent Intensity in %
FRAP without pressure chamber	0.80
FRAP with pressure chamber	0.97
HW without pressure chamber	0.80
HW with pressure chamber	0.80

Comparison w/ and w/o pressure chamber

Figure 7 illustrates the mass flow density measured with the FRAP with and without the pressure chamber installed. The tests are carried out on different days with a significantly different ambient pressure. Therefore, the mass flow density is presented in a normalized form.

Figure 8 shows that the differences in the Mach number with and without the pressure chamber is below 1 %. The difference of Mach number of around ΔMa $\approx$ 0.003 is comparable to results from Gieß et al in [2].
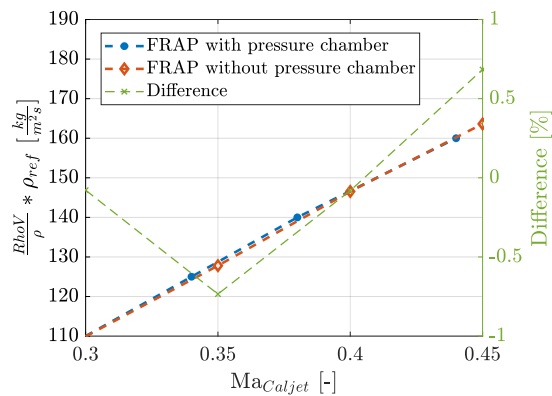
Figure 7. Mass flow density measured with FRAP for different Mach numbers.
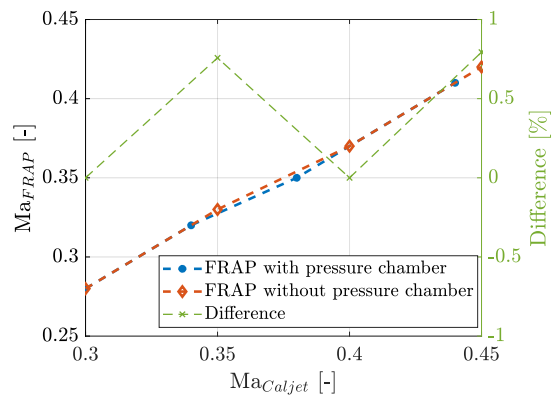

Figure 8. Comparison of Mach number measured with FRAP.

Flow distribution downstream from the nozzle

Figure 9 displays the CFD prediction of the nozzle profile of the Mach number compared to experimental results at throttled conditions. The flow condition is kept stable at a defined static pressure and Mach number. During the test, the pressure distribution inside the flow is measured with a 5HP. The mass flow is set as a boundary condition for the simulation and is calculated from experimental data. The total and static pressure is measured with an accuracy of $\pm 25\,\mathrm{Pa}$ and the total temperature with an accuracy of $\pm 1.5\,\mathrm{K}$. This error leads to a difference in the measured mass flow from $-0.5\,\%$ to $+0.17\,\%$. It can be seen that the behavior of the main flow between simulation and experimental data coincides well. Additionally, the Mach number calculated using the total pressure inside the settling chamber and the static pressure inside the pressure chamber agrees well with the Mach number from the 5HP.

Figure 10 illustrates the pressure distribution inside the pressure chamber. The pressure is normalized by the total pressure inside the settling chamber. The 5HP data is in accordance with the measured values from the Caljet. However, the 5HP data is not reliable in the shear area around the main flow, since the strong velocity gradient leads to problems, this was also observed by Willinger et al in [7]. A slight shift of the static pressure measured by the 5HP compared to the static pressure of the Caljet can be noticed.
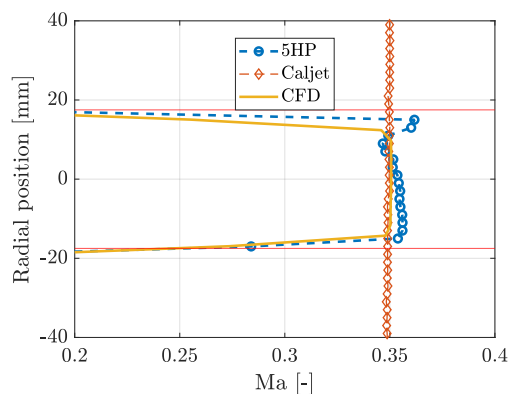

Figure 9. Mach number distribution inside the pressure chamber.
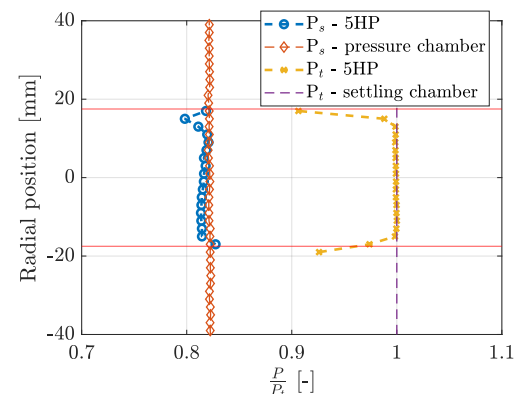

Figure 10. Pressure distribution inside the pressure chamber.

Tests at throttled flow conditions

Firstly, a test is carried out to measure the mass flow density with a HW at constant Mach number Ma = 0.4 but different static pressures. To adjust the flow condition, the total inlet pressure and the degree of throttling is varied. The expected linear behavior between static pressure and mass flow density could be observed during this test.

For further tests, a certain level of throttling is applied while the total pressure is varied. A 5HP is placed 30.9 mm downstream from the nozzle.

Figure 11 shows the mass flow density over the ratio of the static pressure P_s to the ambient pressure P_{amb}. The static pressure inside the pressure chamber is raised to 1.38 times the ambient pressure. The mass flow density of the 5HP is calculated with the temperature measured in the settling chamber. Usually, the total temperature Kiel probe behind the nozzle is used for measuring the flow temperature when using the heater, as a significant heat loss over the throat and nozzle leads to incorrect temperature measurements inside the settling chamber. Since in this test, the flow temperature is close to the ambient temperature and remains stable also in Mach number by using the 13 bar pressure system, the assumption to use the temperature measured in the settling chamber is valid. It can be seen that the measured mass flow density from the 5HP merely displays small deviations compared to the mass flow density measured by the Caljet.

Figure 12 shows the total pressure at different static pressure levels inside the pressure chamber. The measured values from the Caljet and 5HP match well, including for different Mach numbers.
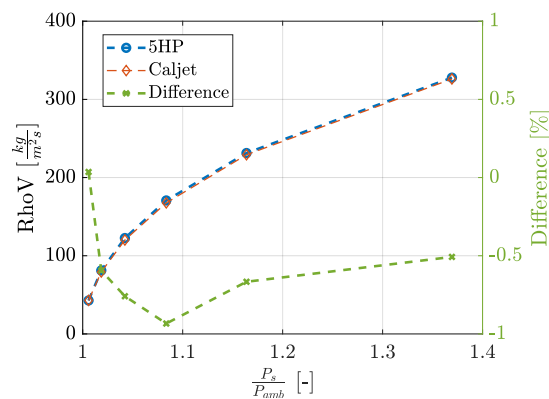

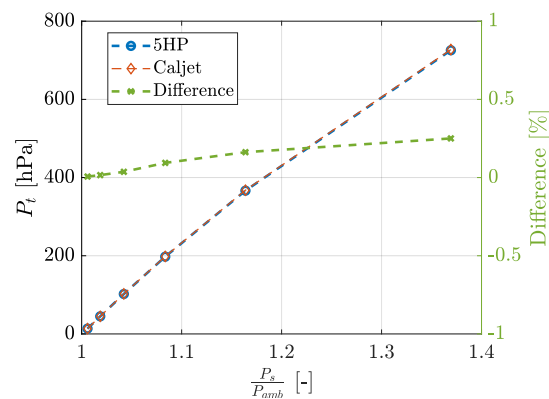**Figure 11.** Mass flow density at varying inlet total pressure.

Figure 12. Total pressure at different pressure levels inside the pressure chamber.

Axial static pressure distribution during probe Reynolds number variation

During this test, the distribution of the static pressure within the pressure chamber is investigated. Therefore, all axial static wall pressure measurements, a pressure probe outside of the core flow and a 5HP inside the core flow are used to evaluate the static pressure distribution. The axial positions are shown in Figure 2.

The test is carried out at a Mach number of Ma = 0.4 and a probe Reynolds number of Re = 24,921 which equals a Reynolds number ratio compared to ambient of $Re_{norm} = \frac{Re}{Re_{ambient}} = 1.8$. The probe Reynolds number is calculated following Equation (2), where v is the flow velocity, ρ the flow density (calculated from static pressure and temperature), and η is the dynamic viscosity.

$$\mathrm{Re}_{probe} = \frac{\rho \cdot v \cdot d_{probehead}}{\eta} \tag{2}$$

Figure 13 shows the measured wall, 5HP, and probe pressures. The horizontal axis corresponds to the measurement position in mm behind the nozzle. It can be seen that the wall pressure is constant and does not change significantly over the first measurement positions. The wall pressure 80 mm behind the nozzle, which is already close to the contraction area connected to the tubing (c.f. Figure 2), indicates lower values.

The horizontal lines represent the two measured probe pressures. To analyze the 5HP static pressure, the coefficients following Schäffer et al [3] are used. The static pressure calculated from the 5HP pressures is significantly lower compared to the wall and pressure probe pressures. Further investigations are necessary to evaluate whether this is a phenomenon driven by the change in the Reynolds number or a problem of the pressure chamber design.

This test was carried out for nine different Reynolds numbers ($\mathrm{Re}_{norm} = 1, 1.1, 1.2, 1.3, 1.4, 1.5, 1.6, 1.7, 1.8$) at the same Mach number $\mathrm{Ma} = 0.4$. An underestimation of the 5HP static pressure and constant axial wall pressure is observed during all tests.

Capability of pressure chamber configuration

Figure 14 and Table 3 illustrate the capability of the calibration wind tunnel in combination with the pressure chamber. The maximum nozzle Reynolds number for different Mach numbers and temperatures is shown. The maximum mass flow density of $RhoV_{max} = 480\,\mathrm{kg/m^2 s}$ is reached at $\mathrm{Ma} = 0.9$ and $T = 293$ K.
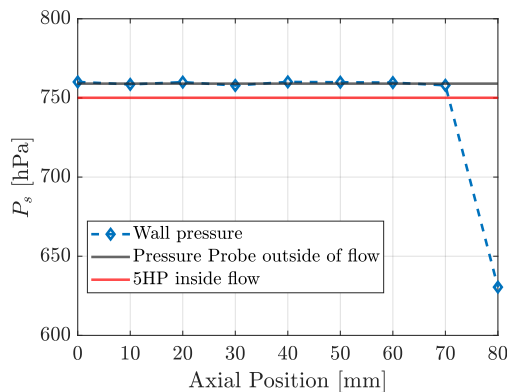

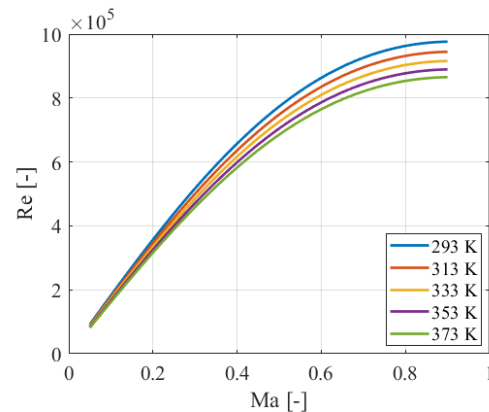**Figure 13.** Static pressure distribution inside pressure chamber.

Figure 14. Capability of new probe calibration tunnel with pressure chamber.

Safety

Since neither the settling chamber nor the pressure chamber is rated for a pressure of 13 bar, a safety mechanism is required. Therefore, two overpressure valves are installed at the settling chamber to release pressure above 1250 hp overpressure. Furthermore, during operations including the pressure chamber, it is not permitted to close the manual throttling valve completely (cf. Figure 5 (5)).

Table 3. Capability of wind tunnel with pressure chamber.

Quantity	Value	Unit
Mach number	$0.02 - 0.95$	-
Calibration static pressure	$amb - 1250$	hPa
Maximum absolute total pressure	2250	hPa
Nozzle diameter	25, 35, 42	mm
Temperature	$293 - 373$	K
Mass flow density	$22 - 480$	$\mathrm{kg/m^2s}$
Nozzle Reynolds number	$8 \cdot 10^4 - 9 \cdot 10^5$	-

5. Outlook and discussion

At the Chair of Turbomachinery and Flight Propulsion at the Technical University of Munich a modification for varying the Reynolds number independent from the Mach number of an existing probe calibration wind tunnel is introduced. The design of a pressure chamber including a throttling system is described. The capability and quality of the design is investigated via numerical simulations and experimental tests. The results show that neither the throttling mechanism nor the pressure chamber itself influences the calibration area in which the probe is located.

The new pressure chamber has the capability to conduct calibrations of HW probes at temperatures between 283 K and 373 K with a mass flow density from 22 $\mathrm{kg/m^2s}$ to 480 $\mathrm{kg/m^2s}$. The Mach number can be varied from Ma = 0.05 to Ma = 0.95. The pressure chamber is used to calibrate HW probes at equal conditions compared to a 3.5-stages axial compressor concept. For further investigations regarding higher static pressures, the pressure chamber will be adapted to a different calibration wind tunnel with a higher pressure rating. Furthermore, the connection to the pressure sensors will be changed to gain a higher pressure ratio capability and to review the numerical results from Schäffer et al in [3] over the entire numerical pressure range.

Nomenclature

5HP	Five-hole probe	D	Diameter
FRAP	Fast Response Aerodynamic Probe	HSRC	High-Speed Research Compressor
HW	Hot-Wire probe	L	Length
LTF	Chair of Turbomachinery and Flight Propulsion	Ma	Mach number
P	Pressure	Re	Reynolds number
RhoV	Mass flow density	s	Static value
T	Temperature	t	Total value
TI	Turbulent Intensity	V	Longitudinal velocity
$\overline{v}\prime$	RMS of turbulent velocity fluctuations		
η	Dynamic viscosity	ρ	Density

References

[1] Boyle R J et al 2002 *Aerodynamic Performance and Turbulence Measurements in a Turbine Vane Cascade Proc. ASME Turbo Expo (Amsterdam)* GT-2002-30434

[2] Gieß P A et al 2000 *A New Test Facility for Probe Calibration - Offering Independent Variation of Mach and Reynolds Number Measuring Techniques in Turbomachinery (Firenze)* GT-2002-30434

[3] Schäffer C et al 2022 *Numerical calibration and investigation of the influence of Reynolds number on measurements with five-hole probes in compressible flows ASME Journal of Turbomachinery* DOI: 10.1115/1.4053835

[4] Eckelmann H 1997 *Einführung in die Strömungsmechanik Springer Fachmedien Wiesbaden GmbH (Wiesbaden)* DOI 10.1007/978-3-663-09882-9

[5] Boufidi E et al 2020 *A Probabilistic Uncertainty Estimation Method for Turbulence Parameters Measured by Hot-Wire Anemometry in Short-Duration Wind Tunnels ASME Journal of Engineering for Gas Turbines and Power* DOI: 10.1115/1.4044780

[6] Hinze J 1975 *Turbulence McGraw-Hill* ISBN-13: 978-0070290372

[7] Willinger R and Haselbacher H 2003 *A Three-Hole Pressure Probe Exposed to Velocity Gradient Effects – Experimental Calibration and Numerical Conference on Modelling Fluid Flow* DOI: 10.1115/1.4044780